Abdominal Radiology

Published online: 18 April 2018

Abdom Radiol (2018) 43:3279–3287
https://doi.org/10.1007/s00261-018-1608-y

Additional value of contrast-enhanced ultrasonography for fusion-guided, percutaneous biopsies of focal liver lesions: prospective feasibility study

Hyo-Jin Kang,[1] Jung Hoon Kim,[1,2] Sang Min Lee,[3] Hyun Kyung Yang,[4] Su Joa Ahn,[1] Joon Koo Han[1,2]

[1]Department of Radiology, Seoul National University Hospital, 101 Daehangno, Jongno-gu, Seoul 110-744, Korea
[2]Institute of Radiation Medicine, Seoul National University College of Medicine, Seoul, Korea
[3]Department of Radiology, Hallym University Sacred Heart Hospital, Anyang, Korea
[4]Department of Medical Imaging, Toronto General Hospital, University of Toronto, Toronto, Canada

Abstract

Purpose: To determine the value of CEUS for real-time, fusion-guided, percutaneous biopsies of focal liver lesions.

Materials and methods: Institutional review board approval and written informed consents were obtained for this study. Forty patients with focal liver lesions identified on CT/MRI were prospectively enrolled. For biopsy planning, real-time fusion of CT/MRI with USG (USG-Fusion) was performed, and subsequently real-time CEUS was fused with CT/MRI (CEUS-Fusion). We evaluated lesion visibility, confidence level of technical success before the procedure, and safety route accessibility on USG-Fusion and CEUS-Fusion. Occurrence of change in the biopsy target was also assessed.

Results: Among 40 target lesions, nine (22.5%) lesions were invisible on USG-Fusion. After applying CEUS-Fusion, seven of nine (77.8%) lesions were visualized. Confidence level of technical success of procedure was significantly increased on CEUS-Fusion compared USG-Fusion ($p = 0.02$), and presumed target lesions were changed in 16 (40%) patients after CEUS-Fusion. As the lesion is necrotic, presumed target was more frequently changed after CEUS-Fusion (50.0% and 25.0%). Confirmative diagnostic results were reported in 39 (97.5%) patients. Accessibility of the safety route to target lesions did not reach statistical differences.

Conclusion: Applying a new, real-time CEUS-Fusion with CT/MRI improved tumor visibility and viable portion assessment, thus leading to higher operator confidence and diagnostic yield, when compared with conventional USG-Fusion.

Key words: Liver—Neoplasm—Biopsy—Ultrasound imaging—Contrast agent

Despite the outstanding improvements in imaging and tumor markers in oncology, the final diagnosis of liver tumor still depends on the histopathologic result. Except for surgical excision, ultrasonography-guided (USG), percutaneous liver biopsy is the gold standard for histopathologic confirmation of liver tumors owing to its real-time capacity, no radiation hazard, and good accessibility. However, the overall accuracy of this method has remained approximately 90% [1, 2]. The reason for the false-negative result of this method is assumed to be due to the small lesion size, poor B-mode lesion visibility, inappropriate lesion localization, and limited evaluation of the viable portion. To improve the diagnostic accuracy, there have been several efforts, such as needle design modification, 3-dimensional reconstruction, and color Doppler guidance liver biopsy [3–5].

Recently, the real-time fusion technique of liver CT/MR and USG has been commonly used for liver biopsies as it is easily accessible and helps to be correlated with CT/MR by moving images simultaneously. Many studies have suggested the advantages of the real-time fusion technique for the percutaneous liver procedure, in terms of the better localization and detecting small or poorly

Correspondence to: Jung Hoon Kim; *email:* jhkim2008@gmail.com

conspicuous lesions [6–8]. If there is picky liver which is bearing multiple nodules and there is only one target lesion and not the others, this technique provides better feasibility and lesion conspicuity by offering landmarks for accurate localization. However, there are still some limitations regarding subcapsular- or subphrenic-located lesions [9]. Also, as the real-time fusion technique is based on B-mode USG image, there are still unmet needs for obtaining accurate liver specimens, especially in patients with isoechoic or necrotic masses.

Likewise, fusion technique, contrast-enhanced ultrasonography (CEUS), has been used to augment USG-guided liver biopsy. The second-generation contrast media are able to make the differential diagnosis and to depict the real-time vascularity of tumors [10]. This property offers not only differentiation of a viable portion in a tumor, but also enhancement distinction from background liver [11]. Many studies have supported the value of CEUS-guided liver biopsy [12–14].

Therefore, when those two novel techniques are used simultaneously, it would be a great advance for more accurate liver biopsy. There are a few studies supporting the value of the combined use of CEUS and the real-time fusion technique for radiofrequency ablation [15, 16]. However, there are a limited number of studies assessing the integrated approach of real-time fusion and CEUS with a prospective design. Therefore, the purpose of our study is to assess the value of the additional use of CEUS to the real-time fusion technique for percutaneous liver biopsy.

Materials and methods

This prospective study was approved by our Institutional Review Board. All patients provided informed consent before their CEUS and biopsy procedure.

Study population

From September 2016 to February 2017, a total of 343 patients were referred to our institution for liver biopsy. Among these patients, 303 were excluded according to one or more of the following exclusion criteria: (a) biopsy for liver parenchyma (n = 108); (b) enrolled in other clinical studies (n = 103); (c) refusal to be enrolled in the study (n = 60); (d) no recent CT or MRI within the past 4 weeks (n = 16); (e) suboptimal image quality (n = 11); (f) hypersensitivity to drugs (n = 3); and (g) a severe heart problem (n = 2). The flow diagram of the patient population is described in Fig. 1. Finally, a total of 40 patients (17 men, 23 women; mean 61 years; age range 34–80 years) with focal liver lesions were prospectively enrolled in this study (Table 1). Twenty-five patients had a history of malignancy in another organ, including the breast (n = 6), gallbladder (n = 5), pancreas (n = 4), cervix (n = 2), ovary (n = 1), bile duct (n = 1), colon (n = 1), esophagus (n = 1), nasopharynx (n = 1), ureter (n = 1), and sex cord (n = 1) or with extramammary Paget's disease (n = 1). Five patients had a history of malignancy in the liver, including hepatocellular carcinoma (n = 3) and intrahepatic cholangiocarcinoma (n = 2). Three patients had liver cirrhosis. Among the study population, two patients had a history of a non-confirmative histologic result of targeted lesions on a conventional, B-mode USG-guided biopsy performed before their study enrollment. All of the patients underwent contrast-enhanced CT (n = 33) or contrast-enhanced MRI (n = 12). The mean time interval between obtaining the images and the biopsy was 14 ± 13.6 days.

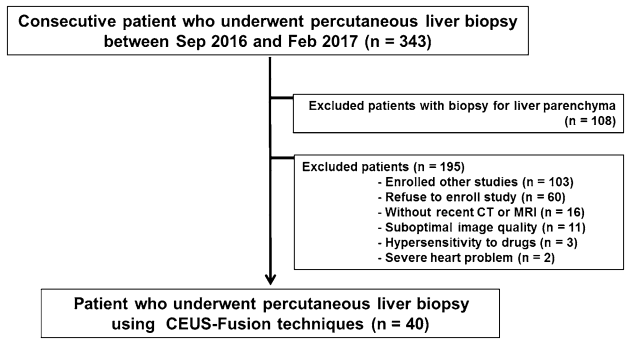

Fig. 1. Flow chart for patient enrollment.

Table 1. Patient demographic data

Age, years (range)	61 (34–80)
Sex	
Male	17 (42.5)
Female	23 (57.5)
Size, cm (range)	3.6 (1.0–8.6)
Histologic biopsy result	
HCC	7 (17.5)
Cholangiocarcinoma	6 (15.0)
Metastasis	21 (52.5)
Eosinophilic abscess	2 (5.0)
GIST	1 (2.5)
Angiosarcoma	1 (2.5)
Neuroendocrine carcinoma	1 (2.5)
Normal liver parenchyma	1 (2.5)

Unless otherwise indicated, data are the number of patients with percentages in parentheses
GIST gastrointestinal stromal tumor

USG with image fusion

For biopsy planning, B-mode USG was performed by one of our three board-certified, abdominal radiologists (H.J.K., S.M.L., H.K.Y.), all of whom with a range of clinical experience in ultrasound imaging of five to 10 years and using conventional USG units (RS80A, Samsung Medison, Seoul, Korea). All of the patients underwent B-mode USG using a 1–7 MHz convex probe (Center frequency of 1.3 MHz; Mechanical index (MI) of 1.3–1.4; gain of 40%–70%; dynamic range of 50; and a frame rate of 26–32 pictures per second) using the

intercostal or subcostal approach. Real-time imaging fusion of CT or MR images with USG (hereafter USG-Fusion) was performed using the vendor-specific fusion algorithm imbedded in the ultrasonography unit (S-Fusion, Samsung Medison, Seoul, Korea).

Imaging fusion was performed using three steps. First, the operator selected the proper CT or MR stack for fusion with a concern regarding lesion and vessel visibility and then sent it to the USG unit via digital imaging communications in medicine data. Second, the probe was placed around the solar plexus in the sagittal plane for the orientation lock. Lastly, for the point lock, the operator selected one of the representative landmarks which are visible on both USG and CT/MR images, such as the right portal vein and its main branches. Point locking was repeated when the imaging fusion is not sufficient. The B-mode and CT or MR image were displayed side-by-side on a USG monitor. The gain and field of view were optimized in order to provide the clearest depiction of the target lesion. For real-time image fusion, the operator selected fusion images according to subjective vessel and lesion visibility. Thirty-one patients with CT (3 late arterial, 22 portal, 6 delayed phases) and nine patients with MR (five portal; four hepatobiliary phase) images were used for image fusion. If there was more than a 1-cm localization difference between the fused USG and the CT/MR images, each dimension, including the axial, sagittal, and coronal planes, was regarded as technical fusion failure.

CEUS with image fusion

Real-time SonoVue (sulfur hexafluoride microbubble, Bracco, Milan, Italy) contrast-enhanced USG fused with CT or MR images, hereafter expressed as CEUS-Fusion, was performed in all patients. After USG-Fusion evaluation, the conventional B-mode was switched to the CEUS mode in the same 1–7 MHz convex probe, and real-time imaging fusion of CT or MR images was sustained. CEUS images were obtained using a contrast harmonic image mode with the following parameters: center frequency of 2.4 MHz; MI of 0.08; gain of 50%–70%; dynamic range of 50; and a frame rate of 9–12 pictures per second. CEUS-Fusion images were also displayed side-by-side on the USG monitor.

The contrast agent was prepared according to the manufacturer's recommendations, and one vial with 4.8 mL was divided into two doses of 2.4 mL each. The first dose was used for pre-biopsy planning, and the second dose was used for biopsy by a manual bolus injection followed by a flush with 10 mL of normal saline via the ante-cubital venous line in each administration. In the first dose of contrast agent injection, continuous CEUS images were obtained under normal, calm breathing for 150 s for target site and route determining [11]. After pre-biopsy planning, USG swapping with high MI was performed for microbubble degradation. A second dose of contrast agent was injected for lesion visualization while on the biopsy site. As most of target lesions (90%, 36/40) presented washout in portal or late phase (Table 2), biopsies for those lesions were performed at 2–3 min after contrast media injection. Among the lesion without washout, two lesions showed rim enhancement in arterial phase; therefore, biopsies for those lesions were performed within 1 min after contrast media injection. For other two lesions which were presented iso-vascularly in all phase, biopsies were performed based on real-time imaging fusion with CT or MRI.

Biopsy technique

All biopsy procedures were performed by one of three board-certified, abdominal radiologists (H.J.K., S.M.L., H.K.Y.) whose clinical experience was with at least 150 cases of percutaneous liver biopsy. Before the biopsies, ascites tapping was performed if needed ($n = 4$) in order to reduce the risk of post-procedural bleeding. After the fusion-based biopsy planning, the biopsy was performed using an 18-gauge, automated, side-cutting biopsy needle (Acecut, TSK laboratory, Tochigi, Japan) with the free-hand technique and with the patient under local anesthesia using 2% lidocaine hydrochloride. We obtained at least two biopsy specimens and repeated sampling was performed if visual inspection of the specimen was doubtful of the technical success.

On-site analysis

Before the procedure, the lesion size and necrosis degree, i.e., grade 0, no necrosis; grade 1, $< 30\%$ necrosis; grade 2, 30%–60% necrosis; and grade 3 $> 60\%$ necrosis, were assessed on CT or MR images. During the procedure, the biopsy operator assessed the necrotic degree in USG-Fusion and in CEUS-Fusion images also assessed using the same scale.

Just before the procedure, the biopsy operator evaluated the lesion subjective visibility using the binary scale and confidence level of technical success using the four point scale, i.e., score 1, low, $< 30\%$; score 2, moderate, 30%–60%; score 3, high, 60%–90%; and score 4 highest, $> 90\%$ and the safety route accessibility, i.e., score 1, bad safety route, unavoidable segmental branches of the portal vein (PV) or hepatic vein (HV); score 2, adequate route, unavoidable small PV or HV branches; and score 3, safe route, no unavoidable large vessel on USG-Fusion or CEUS-Fusion. The occurrence of change in the biopsy target and the overall technical success regarding the image fusion and CEUS application were also evaluated.

Statistical analysis

All values were expressed as mean ± standard deviation (SD). The confidence level of technical success and the safety route assessment were compared using analysis of variance (ANOVA) and post hoc analysis. A p value of < 0.05 was considered to constitute a statistically significant difference. All statistical analysis was performed using commercially available software (SPSS version 22, IBM Corporation, Armonk, NY, USA).

Results

The mean lesion size was 3.6 cm (SD 2.16 cm; range 1.0–8.6 cm). There were no post-procedural complications. Among the 40 patients, four were regarded as having technical failure for accurate image fusion, as the liver orientation had been changed by ascites drainage ($n = 3$) or tilting their body in order to achieve the shortest approach during the biopsy procedures ($n = 1$). However, all of the CEUS examinations were successfully performed. Confirmative histologic diagnostic results were reported in 39 patients (97.5%). Thirty-seven lesions were confirmed as malignancies: metastasis ($n = 21$); hepatocellular carcinoma ($n = 7$); cholangiocarcinomas ($n = 6$); angiosarcoma ($n = 1$); neuroendocrine carcinoma ($n = 1$); and gastrointestinal stromal tumor ($n = 1$). Three lesions were reported to be benign, i.e., two eosinophilic abscesses ($n = 2$) and one normal liver parenchyma ($n = 1$). The histopathologic result of the eosinophilic abscesses presented in concordance with the clinical and imaging features, i.e., one patient with a 23% serum eosinophil level with toxocariasis antigen positive and another patient with a 6.5% serum eosinophil level. All of the patient demographic data and histologic diagnoses are noted in Table 1.

CEUS enhancement patterns of target lesions are summarized in Table 2. In arterial phase, lesions presented various enhancement patterns: hypo-vascular ($n = 12$), iso-vascular ($n = 9$), hyper-vascular ($n = 12$), and rim enhancement ($n = 7$). Most lesion (90%, 36/40) showed washout in portal phase ($n = 27$) or late phase ($n = 9$). Only two lesions showed iso-enhancement in arterial, portal, and late phases.

Among 40 target lesions in 40 patients, nine (22.5%) lesions were invisible on USG-Fusion. Three of the nine invisible lesions were infiltrative masses and which lead to poor demarcation between the tumor and the parenchyma on B-mode USG. Six of the nine invisible lesions were small, i.e., less than 1.5 cm, and were isoechoic on B-mode USG. After applying the CEUS-Fusion, seven of the nine (77.8%) focal, hepatic lesions were visualized (Fig. 2). All seven lesions were showed early washout (within 60 s) and most apparent in late phase (2–3 min after contrast media administration). Among seven lesions, six lesions were metastasis and one lesion was eosinophilic abscess.

The confidence level of technical success before the procedure is, therefore, significantly increased on CEUS-Fusion compared USG-Fusion ($p = 0.02$, Fig. 3). Table 3 summarizes the confidence level of the technical success and safety route assessment in each step. The presumed target point was changed in 16 of 40 (40%) patients after CEUS-Fusion in order to avoid necrotic tissue ($n = 12$) or to select a more visible target on CEUS ($n = 4$). However, accessibility of the safety route to the target lesion did not reach statistically significant differences between USG-Fusion and CEUS-Fusion ($p = 0.67$). If the lesion was necrotic on pre-procedural CT/MR image evaluation, the presumed target lesions were more frequently changed after CEUS-Fusion (50%, 12 of 24, necrotic masses; 25.0%, four of 16, non-necrotic masses, $p = 0.11$, Fig. 4) than in non-necrotic lesions. Table 4 summarizes the occurrence of target site change after CEUS-Fusion during biopsy, according to the necrotic degree. Thirteen patients (32.5%) were not matched with necrotic degrees on CEUS-Fusion and the CT/MR image. Eight patients (20%) presented higher necrotic degrees on CEUS-Fusion, and five patients (12.5%) presented lower necrotic degrees on CEUS-Fusion than on the CT/MR image.

Table 2. CEUS enhancement patterns of target lesion

Arterial enhancement pattern	Washout pattern in portal or delay phase			Total
	No	Early (< 60 s)	Late	
Hypo	0	12	0	12
Iso	2	5	2	9
Hyper	0	5	7	12
Hyper (rim)	2	5	0	7

Discussion

In our study, after applying the CEUS-Fusion, seven of nine (77.8%) lesions were visualized. The confidence level of technical success was significantly increased on CEUS-Fusion compared USG-Fusion ($p = 0.02$). The target lesion was changed in 16 of 40 (40%) patients after CEUS-Fusion. If the lesion was necrotic, the presumed target lesions were more frequently changed after CEUS-Fusion (50%, 12 of 24 necrotic masses; 25.0%, four of 16 non-necrotic masses). Applying a real-time CEUS-Fusion with CT/MR improved the tumor visibility and the viable portion assessment and led to a higher operator confidence and diagnostic yield, compared with conventional USG and real-time CT/MRI fusion.

Among the several technical improvements increasing the success rate of percutaneous liver procedures, the real-time fusion technique of liver CT/MR and USG has been gaining great attention due to its easy accessibility and better lesion localization [8, 9]. Park et al. suggested

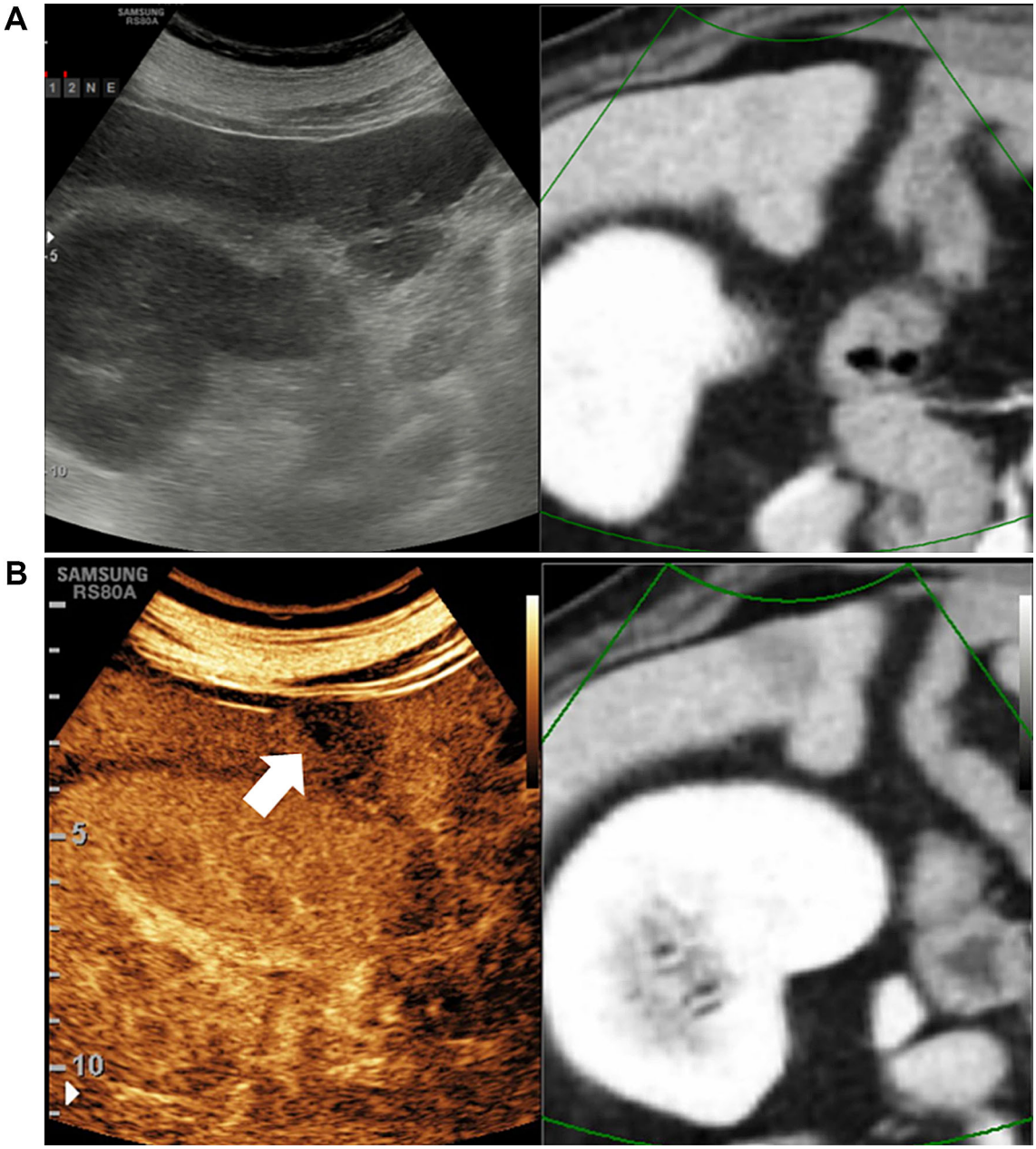

Fig. 2. Examples of USG and USG-Fusion invisible lesion. A 75-year-old male with common bile duct cancer presented a low attenuating lesion at segment 6. The lesion is invisible on conventional USG and USG-Fusion (**A**). When the CEUS is added on Fusion image (**B**), the S6 lesion is visible (white arrow) and confirmed as CBD cancer metastasis.

the effectiveness of fusion imaging for percutaneous biopsies of poorly conspicuous lesions on USG [6]. Even in lesions poorly conspicuous on USG, the perilesional, anatomic landmarks seen on fusion imaging guide accurate lesion localization. In cases of intractable, liver-bearing, multiple nodules in which there is only one target lesion and the others are not, this technique provides better feasibility and lesion conspicuity by offering landmarks for accurate localization. However, the real-time fusion technique has inherent limitations regarding misregistration [9]. If a lesion is located peripherally and at a distance from landmarks, a small difference between fused images in the central portion of the liver could actually be a large difference. Also a patient's heartbeat or breathing motion gives rise to misregistration. Similarly, in our study there are four misregistration cases regarded as technical failure due to the change of liver orientation after ascites drainage ($n = 3$) or the tilted body in order to achieve the shortest approach during the biopsy procedures ($n = 1$). In our study, nine (22.5%) lesions were invisible on USG-Fusion. Three of the nine invisible lesions were infiltrative masses which

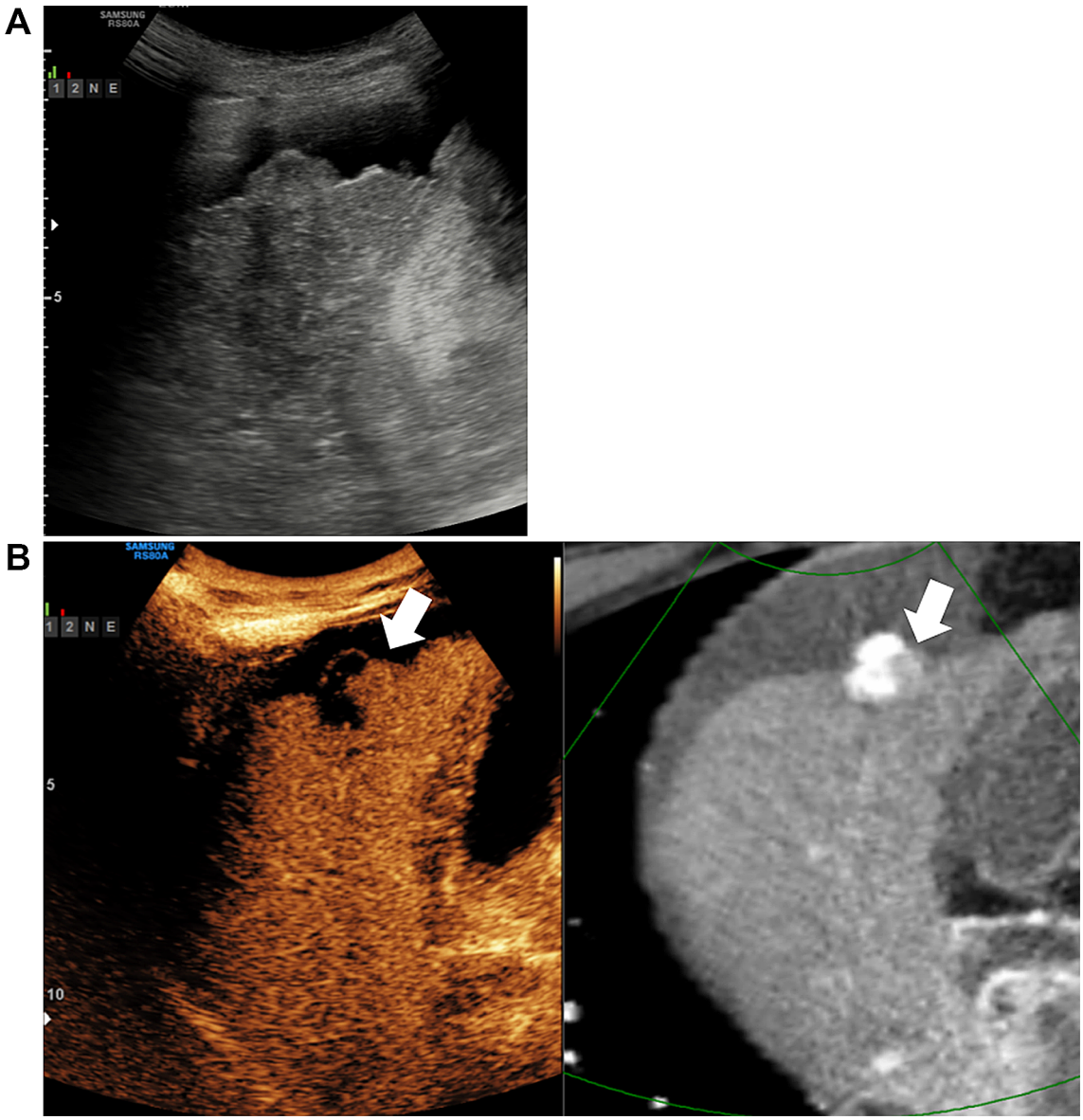

Fig. 3. A 61-year-old male with history of multisession TACE for HCC. On CT image, there was suspicious marginal recurrence on segment 5 lipiodolized nodule (**B**, white arrow). But on conventional USG, the viable portion is not distinguished from lipiodol (**A**). When the CEUS is added, the lipiodol and viable portion (white arrow) is clearly distinguished.

Table 3. Confidence level of technical success and safety route assessment in each step

	USG-Fusion	CEUS-Fusion	*p*
Confidence level of technical success	3.0 (1.1)	3.6 (0.82)	0.02
Safety route accessibility	2.6 (0.60)	2.6 (0.63)	0.67

Data in parentheses are standard deviation

led to poor demarcation between tumor and parenchyma on B-mode USG. Six of the nine invisible lesions were small, i.e., less than 1.5 cm, and were isoechoic on B-mode USG. After applying the CEUS-Fusion, seven of the nine (77.8%) focal, hepatic lesions were visualized.

Likewise, the fusion technique, CEUS, can be used for poorly conspicuous target lesions during percutaneous liver procedures and many studies have supported this [12–14, 17]. Recently, Francica G et al. reported the effect of CEUS on challenging liver biopsy case in multicenter bases [18]. The results were similar to our results. Wei Wu et al. also reported that CEUS-guided liver biopsy provides intra-lesional information for the viable portion and thus results in more accurate biopsy results even in small lesions (< 2.0 cm) [14]. Owing to the development of second-generation, blood-pool sono-

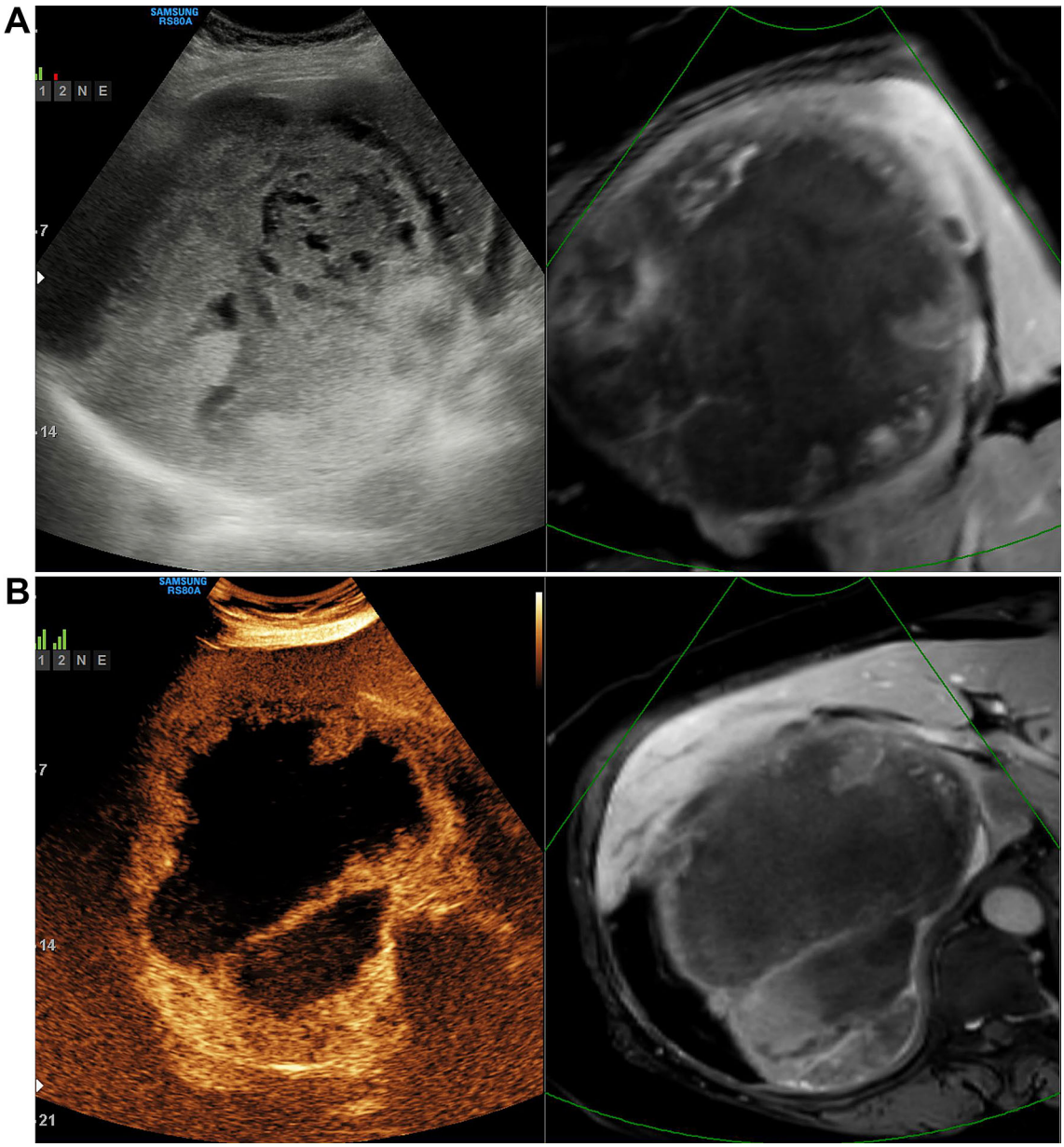

Fig. 4. A 63-year-old female with large necrotic liver mass. On conventional USG, hyperechoic necrotic debris in the lesion mimic viable portion (**A**). (**B**) By adding CEUS on real-time fusion image, viable portion is clearly distinguished from necrotic portion. The specimen is obtained peripheral viable portion and diagnosed as GIST.

Table 4. The incidence of target site change after CEUS-Fusion during biopsy according to the necrotic degree

Necrosis degree (%)*	Patients number	Target change
0	16	4 (25%)
< 30	14	7 (50%)
30–60	8	4 (50%)
> 60	2	1 (50%)

*Necrotic degree of target lesion was assessed in CT or MR image

graphic contrast media, it lasted through all of the dynamic phase [19]. This property makes it possible to obtain on-site characterization of a lesion [10, 20] and visualization of a poor conspicuity lesion using the distinct enhancement pattern of background liver [11, 21]. Also, in necrotic lesions, this cannot be easily identified on conventional sonography before liquefaction has occurred [22]. Likewise, in our study, when a lesion was necrotic, the presumed target lesions were more frequently changed after CEUS-Fusion (50%, 12 of 24 necrotic masses; 25.0%, four of 16 non-necrotic masses). In our study, thirteen patients (32.5%) were not matched with necrotic degrees on CEUS-Fusion and the CT/MR image. Although it is hard to explain the reason of this mismatch between CEUS and CT/MRI, one of possible

reasons is different mechanisms of contrast agents. US contrast is retained only within the blood vessels; on the contrary, CT/MRI contrast agent moves into the extracellular space.

In such a situation, CEUS can be mutually complementary with the real-time fusion technique, especially in poorly conspicuous lesions. The better lesion localization identified by the fusion technique and the better conspicuity by CEUS could be a good supporters of each other [16, 23]. In our study, not only seven of nine invisible lesions became visible after CEUS application, but also in two invisible cases even after CEUS application, the biopsy results were confirmative owing to the guidance of the real-time fusion technique. The operator confidence level also significantly increased. Kang et al. [24] reported that 15 of 16 (93.8%) invisible lesions become visible by applying CEUS under fusion imaging guidance. However, CEUS was only used in USG invisible lesions and was not included in necrotic masses, which is another good indication of CEUS-Fusion application in percutaneous liver biopsies.

Of course, we have to consider the cost-effectiveness of additional use of USG contrast media not only the price but also the time consumption. Indeed, biopsy targeting points were not changed in 24 patients even after contrast media administration in our study. Therefore, in the real practice, dedicated selection for USG contrast media usage in liver biopsy is crucial, such as necrotic or invisible lesion on B-mode USG.

Our study had several limitations. First, there is no control group comparison. Therefore, the diagnostic yield differences between the USG-Fusion and the CEUS-Fusion groups cannot be assessed. According to a previous study, the diagnostic yield of USG-guided liver biopsy is approximately 90% [1, 2] and it was 97.5% in our study. Also, the average diagnostic yield of USG-Fusion-guided liver biopsy at our institution is approximately 94% without CEUS application. Secondly, our study population was small. Even though there is a tendency toward more target point change in necrotic masses than in non-necrotic masses, in our study there were no statistically significant differences. Further study on a large number of patients is needed to validate this. However, our results are meaningful as to date there have been a limited number of studies assessing the integrated approach of real-time fusion and CEUS with a prospective design.

In conclusion, applying a new, real-time, CEUS-Fusion using CT/MRI improved the tumor visibility and viable portion assessment and led to a higher operator confidence and diagnostic yield compared to conventional USG and real-time CT/MRI fusion.

Acknowledgements We also thank Bonnie Hami, M.A. (USA) for her editorial assistance in the preparation of this manuscript.

Compliance with ethical standards

Funding This research was partially supported by a research grant from SAMSUNG MEDISON Co., Ltd. and by a research grant from the Basic Science Research Program through the National Research Foundation of Korea (NRF) funded by the Ministry of Science, ICT & Future Planning (2017R1A2B4004951).

Conflict of interest Jung Hoon Kim has received research grant from SAMSUNG MEDISON. Other authors confirm that there are no potential conflicts of interest to disclose.

Ethical approval All procedures performed in studies involving human participants were in accordance with the ethical standards of the institutional and/or national research committee and with the 1964 Helsinki declaration and its later amendments or comparable ethical standards.

Informed consent Informed consent was obtained from all individual participants included in the study. This prospective study was approved by our Institutional Review Board. All patients provided informed consent before their CEUS and biopsy procedure.

References

1. Elsayes KM, et al. (2011) Diagnostic yield of percutaneous image-guided tissue biopsy of focal hepatic lesions in cancer patients. Cancer 117(17):4041–4048
2. Francque S, et al. (2002) Biopsy of focal liver lesions: guidelines, comparison of techniques and cost-analysis. Acta Gastro-enterologica Belgica 66(2):160–165
3. Lencioni R, Caramella D, Bartolozzi C (1995) Percutaneous biopsy of liver tumors with color Doppler US guidance. Abdom Imaging 20(3):206–208
4. Polaków J, et al. (2003) Value of three-dimensional sonography in biopsy of focal liver lesions. J Hepato-Biliary-Pancreatic Sci 10(1):87–89
5. Diederich S, et al. (2006) Application of a single needle type for all image-guided biopsies: results of 100 consecutive core biopsies in various organs using a novel tri-axial, end-cut needle. Cancer Imaging 6(1):43
6. Park HJ, et al. (2013) Fusion imaging–guided percutaneous biopsy of focal hepatic lesions with poor conspicuity on conventional sonography. J Ultrasound Med 32(9):1557–1564
7. Jung E, et al. (2009) New real-time image fusion technique for characterization of tumor vascularisation and tumor perfusion of liver tumors with contrast-enhanced ultrasound, spiral CT or MRI: first results. Clin Hemorheol Microcirc 43(1–2):57–69
8. Lee MW, et al. (2013) Planning US for percutaneous radiofrequency ablation of small hepatocellular carcinomas (1–3 cm): value of fusion imaging with conventional US and CT/MR images. J Vasc Interv Radiol 24(7):958–965
9. Lim S, et al. (2014) Mistargeting after fusion imaging-guided percutaneous radiofrequency ablation of hepatocellular carcinomas. J Vasc Interv Radiol 25(2):307–314
10. Quaia E, et al. (2004) Characterization of focal liver lesions with contrast-specific US modes and a sulfur hexafluoride–filled microbubble contrast agent: diagnostic performance and confidence. Radiology 232(2):420–430
11. Claudon M, et al. (2013) Guidelines and good clinical practice recommendations for contrast enhanced ultrasound (CEUS) in the liver–update 2012. Eur J Ultrasound 34(01):11–29
12. Yoon SH, et al. (2010) Real-time contrast-enhanced ultrasound-guided biopsy of focal hepatic lesions not localised on B-mode ultrasound. Eur Radiol 20(8):2047–2056
13. Sparchez Z, et al. (2011) Usefulness of contrast enhanced ultrasound guidance in percutaneous biopsies of liver tumors. J Gastrointestin Liver Dis 20(2):191–196
14. Wu W, et al. (2006) The role of contrast-enhanced sonography of focal liver lesions before percutaneous biopsy. Am J Roentgenol 187(3):752–761
15. Min JH, et al. (2014) Radiofrequency ablation of very-early-stage hepatocellular carcinoma inconspicuous on fusion imaging with

B-mode US: value of fusion imaging with contrast-enhanced US. Clin Mol Hepatol 20(1):61
16. Minami T, et al. (2014) Combination guidance of contrast-enhanced US and fusion imaging in radiofrequency ablation for hepatocellular carcinoma with poor conspicuity on contrast-enhanced US/fusion imaging. Oncology 87(Suppl 1):55–62
17. Bang N, et al. (2000) Clinical report: contrast enhancement of tumor perfusion as a guidance for biopsy. Eur J Ultrasound 12(2):159–161
18. Francica G et al. (2017) Biopsy of liver target lesions under contrast-enhanced ultrasound guidance-a multi-center study. Ultraschall in der Medizin (Stuttgart, Germany: 1980)
19. Solbiati L, et al. (2001) The role of contrast-enhanced ultrasound in the detection of focal liver leasions. Eur Radiol 11:E15–E26
20. Catalano O, et al. (2005) Real-time harmonic contrast material–specific US of focal liver lesions. Radiographics 25(2):333–349
21. Schlottmann K, et al. (2004) Contrast-enhanced ultrasound allows for interventions of hepatic lesions which are invisible on convential B-mode. Zeitschrift für Gastroenterologie 42(04):303–310
22. Solbiati L, et al. (2004) Guidance and monitoring of radiofrequency liver tumor ablation with contrast-enhanced ultrasound. Eur J Radiol 51:S19–S23
23. Jung EM, et al. (2012) Volume navigation with contrast enhanced ultrasound and image fusion for percutaneous interventions: first results. PLoS ONE 7(3):e33956
24. Kang TW, et al. (2017) Added value of contrast-enhanced ultrasound on biopsies of focal hepatic lesions invisible on fusion imaging guidance. Korean J Radiol 18(1):152–161